An Automatic Light Scattering CCN Counter

G. G. LALA AND J. E. JIUSTO

Atmospheric Sciences Research Center, State University of New York, Albany 12222

(Manuscript received 7 January 1976, in revised form 1 March 1977)

ABSTRACT

An automatic instrument for the measurement of cloud condensation nucleus (CCN) concentrations utilizing a thermal gradient diffusion chamber and light scattering has been developed. The concentration of droplets (activated CCN) in an illuminated volume is determined by the measurement of the peak light intensity scattered at 45°. The CCN concentration is linearly related to the scattered light signal at a fixed supersaturation S, but the sensitivity exhibits an $S^{0.55}$ dependence over a range of supersaturations. Calibration of the system against the photographic method verifies the linear dependence of scattered light on number concentration. The main features of the system are the automatic sampling, measurement and recording of CCN droplet concentration by means of scattered light with the capability of direct calibration by means of the photographic method. Results from four days of continuous hourly measurements of the CCN spectra show the influence of meteorological events on CCN. Included in the data are a frontal passage, fog formation and dissipation, and the occurrence of a nocturnal peak.

1. Introduction

The static thermal diffusion chamber has been used extensively for the measurement of cloud condensation nucleus (CCN) concentrations. This technique offers the capability of accurately prescribing supersaturations which can be varied over the range of values encountered in clouds. In most systems utilizing the static diffusion chamber, the concentration of droplets is measured by photographing a carefully defined illuminated volume and subsequently counting the bright spots on the film. This is not only tedious and time consuming, but limits the amount of information that can be obtained on time and spatial variations of CCN concentrations. The time involved in this procedure precludes real-time analysis of CCN variations. One approach to overcoming this problem is the system designed by Radke and Hobbs (1969) in which the number concentration of droplets is determined from a measurement of the extinction coefficient of the droplet cloud when most of the drops have reached a size corresponding to the first Mie peak. Twomey and Davidson (1970) have continuously operated a conventional static chamber such that air samples are drawn and photographs automatically taken at approximately hourly intervals. Interesting diurnal and seasonal trends have been indicated, but the subsequent data analysis of such a procedure is formidable.

The method to be described in this paper allows for the determination of the droplet concentration from scattered light measurements while preserving the features of the usual static diffusion chamber design. The instrument has been developed to the state where it can operate unattended for long periods of time providing measurements of CCN supersaturation spectra.

A similar automatic scattering instrument was developed by Mee Industries, Inc., of Los Angeles. It came to our attention in December 1972 during the early stages of development of this system. The portable Mee instrument uses the same light scattering principle discussed in this paper and also performs its functions automatically. Features of our instrument include the method of calibration, the illumination system, and the proven capability of unattended operation over a range of supersaturations. Mee Industries was not aware of the fundamental drop concentration (and calibration) dependence on supersaturation—items now reportedly accounted for based on this work.

2. Design principles

When observing a volume of the chamber illuminated by a tungsten lamp with a photodetector directed to measure light scattered in a forward direction, the scattered light signal is observed to rise to a peak and then fall off with time during a sampling sequence. The initial increasing signal is due to the rapid growth of the droplets to near uniform size, and the eventual decline is due to the removal of droplets by sedimentation. The magnitude of this peak scattered light signal is directly proportional to the number concentration of droplets.

The use of a continuous spectrum light source such as a tungsten lamp results in a smoothing of phase effects in the scattered light signal, and the Mie peaks

generally are not evident in the signal. This has been verified by recording the scattered light intensity as a function of time for many samples at several supersaturations. The use of a forward scattering angle of 45° with tungsten illumination insures that the scattering intensity coefficient for the drop sizes involved is reasonably constant (Hodkinson and Greenfield, 1965). The first Mie peak corresponds to a drop radius of ~ 0.5 μm for the light source involved. Most all drops rapidly exceed this size at chamber supersaturations (S) $\geqslant 0.5\%$. At lower supersaturations drop sizes become progressively less uniform and smaller such that some variations in drop scattering intensity might be expected. For these reasons, our adopted minimum supersaturation is 0.25%. Conventional static chambers possess a practical lower limit of 0.1–0.2% because of the difficulty in differentiating haze and effective CCN droplets (Twomey, 1967; Squires, 1972).

The following simplified theory will illustrate how the effects of droplet growth, sedimentation and light scattering combine to produce the linear relationship between the peak scattered intensity and the droplet concentration.

We will tentatively assume a simplified droplet growth equation of the form

$$r\frac{dr}{dt}=GS, \tag{1}$$

where r is the droplet radius, t the time, S the supersaturation, and G a thermodynamic constant. The effect of a size distribution is neglected because it can be shown that the growing droplets tend to a monodisperse distribution, particularly at the higher supersaturations as mentioned. The effects of curvature and dissolved salt have been omitted for simplicity, but are discussed later. The particles are assumed to fall at a velocity given by Stoke's law, i.e., by

$$V=Br^2, \tag{2}$$

where V is the fall velocity and B a constant. The collimated beam of light has a rectangular cross section 0.5 cm high and 0.2 cm wide. If we assume an illuminated volume of the chamber with a rectangular cross section and height h initially containing a number of drops N_0 which all have the same growth rate and commence to fall uniformly, then we can write the following equation for the number of drops N in the volume as a function of time:

$$\frac{dN}{dt}=\frac{-VN_0}{h}. \tag{3}$$

While there is some flux of drops into the top of the illuminated volume, their contribution to the scattered light signal is small in comparison to the larger uniform drops in the central and lower part of the beam. Within the framework given, the scattered intensity can be written as

$$I=CNr^2, \tag{4}$$

where I is the scattered intensity and C a constant containing the incident illumination, the scattering intensity coefficient, and various geometric factors influencing the signal magnitude.

Eqs. (1)–(4) may be integrated to give expressions for the droplet concentration and for the scattered light intensity as a function of CCN concentration and supersaturation as follows:

$$N=N_0\left(1-\frac{BGSt^2}{h}\right), \tag{5}$$

$$I=C2GSN_0t\left(1-\frac{BGSt^2}{h}\right). \tag{6}$$

From expression (6) we can find the time of occurrence of the peak scattered light which is

$$t_m=\left(\frac{h}{3BGS}\right)^{\frac{1}{2}}. \tag{7}$$

Eqs. (6) and (7) can be combined into an expression for the peak scattered intensity

$$I_p=C\tfrac{4}{3}G\left(\frac{h}{3BG}\right)^{\frac{1}{2}}S^{\frac{1}{2}}N_0, \tag{8}$$

which predicts that the peak value is a function of only the initial droplet concentration and the supersaturation. Also of importance is that the time of occurrence of the peak is a function of supersaturation alone; and [from (5) and (7)] the number of droplets at the time of the peak is two-thirds of the initial concentration, independent of supersaturation.

A fairly complete model of the development of drop size distribution in a thermal gradient diffusion chamber has been reported by Alofs and Carstens (1976). Their results show large differences in the drop size distribution as a function of the slope k of the CCN spectra as well as the operating supersaturation; large errors in the photographic counting accuracy can ensue depending on the detection limit for a particular optical system. These results led us to develop a similar computer model of the chamber performance with the additional consideration of the light scattered by the droplets growing on hygroscopic nuclei.

The results of the model computations confirm that the peak scattered light signal is linearly related to the CCN concentration at a given supersaturation and for a fixed value of the slope of the CCN spectrum. The average predicted dependence of the scattered light signal on supersaturation was a power law with an exponent of 0.57 compared with a value of 0.5 predicted

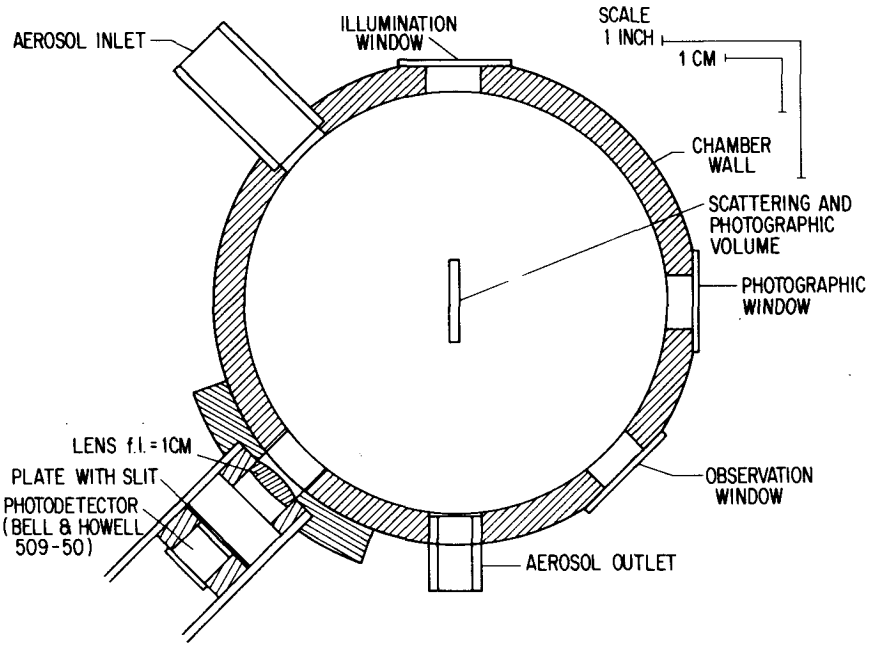

FIG. 1. Schematic diagram of the static diffusion chamber showing the location of the scattering volume with respect to the illumination window, photographic window and the scattered light measurement system.

by the simple theory. Some dependence of the S exponent on the slope of the CCN spectra was found which results in a deviation of ± 0.1 from the average k exponent predicted by the model. Details of these computations will be reported in a separate publication.

3. Apparatus

a. Thermal diffusion chamber

The thermal diffusion chamber is a cylindrical volume with an aspect ratio of 9.5 and a height of 0.8 cm. Aluminum plates of 0.7 cm thickness form the top and bottom of the chamber. These plates are covered with blotter paper which is kept wet by a system of holes and channels connected to a water reservoir. The wall of the chamber is a plexiglass ring of 1 cm thickness.

The temperature of the bottom plate is controlled by means of a thermoelectric cooler which forms part of a closed loop temperature regulator. Upper and lower surface temperatures are sensed with linear thermistor composites with differential accuracies of 0.1°C. The closed loop temperature regulator is capable of maintaining the temperature difference between the upper and lower surfaces to within ± 0.05°C of preset values over long periods of time, making it possible to accurately prescribe the supersaturation.

The chamber was originally designed to operate as a conventional system with provision for photographic recording of the droplets. All of the elements of this system have been preserved with the exception of a change in the light source from a 100 W mercury-arc lamp to a 150 W tungsten lamp. This change was made necessary by the choice of a silicon photodetector for the scattered light sensor which has much higher sensitivity at longer wavelengths. Also, continuous operation is difficult with the mercury lamp because of its short lifetime and changing characteristics with age. The lamp is operated at full power only for 30 s of each measurement (next section) to prolong lamp life and to eliminate any chamber heating effect.

A collimated beam formed by the first lenses in the optical system illuminates a carefully machined slit which is imaged in the center of the chamber by a second lens. A section of the resultant rectangular ribbon of light (0.2 cm $\times$ 0.5 cm, dimensions noted earlier) of length 1.5 cm is sufficiently well defined to prescribe the illuminated volume for photography. This volume is also the sensitive volume for the light scattering measurement. Recording of the droplets is accomplished by photographing the illuminated volume at a right angle with a modified oscilloscope camera using polaroid film.

b. Scattered light detector

Components of the scattered light detection system are a simple lens, a slit and an integrated silicon photodetector-amplifier. As shown in Fig. 1, the photodetector system looks at the previously described scattering volume from a forward scattering angle of 45°. The lens serves to provide a large collection aperture and focuses the image of the droplet cloud on a slit carefully machined to eliminate light from sources other than the scattering volume. Located immediately behind the slit is the photodetector which

collects the scattered light and provides a voltage output which is a linear function of the incident intensity.

c. Operating systems

The operating system for controlling the air flow and electro-optics circuits consists of a time sequence generator, peak sample hold circuits and an output multiplexor. A typical cycle of operation begins with a 5 s sample period during which the chamber is purged,

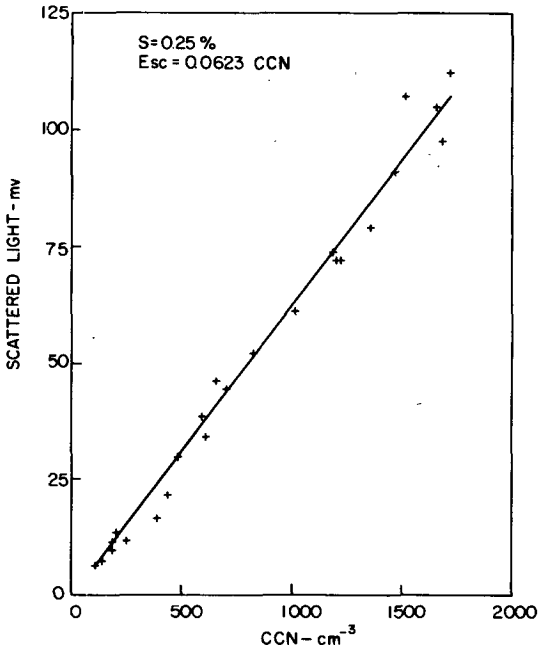

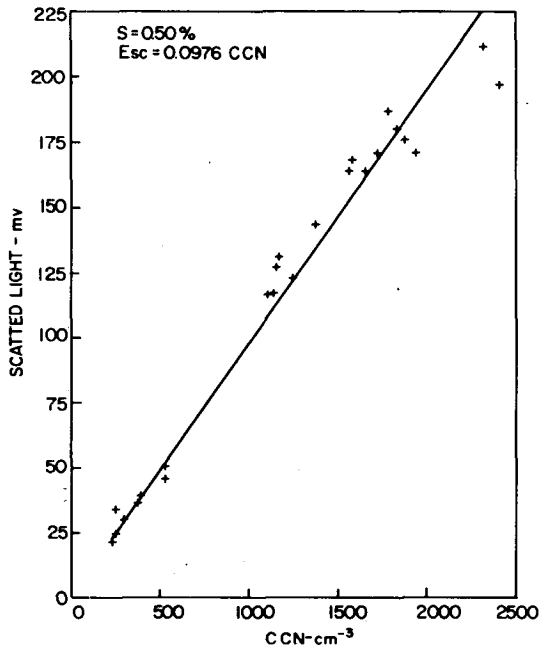

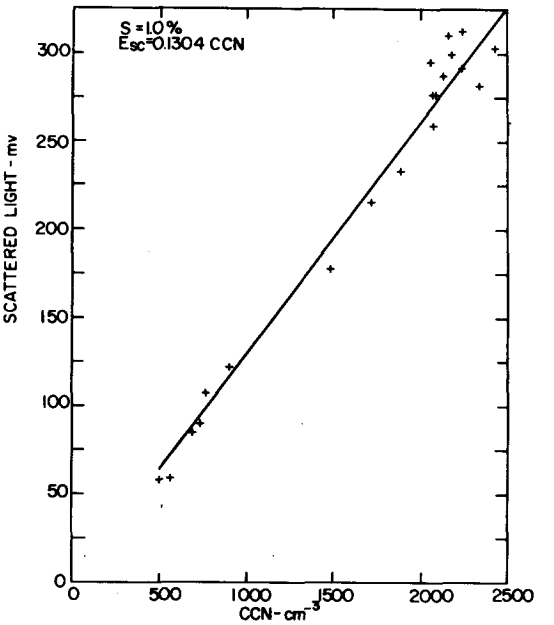

FIG. 2. Calibration curves at three supersaturations [(a)–(c)] showing scattered light signal E_{sc} versus photographic count.

the lamp intensity is raised from standby to full power, and the peak sample hold circuits are reset to the level of the background scattered light as indicated by the photodetector. Following the sampling period is a 25 s interval during which the cloud forms and the scattered light peak is recorded by the peak sample hold. (The time of 25 s was chosen to conservatively exceed the time for peak cloud formation at the lowest supersaturation employed.) At the end of this cycle, the lamp intensity is reduced to the standby level. During the last part of the cycle, the top plate temperature signal and the temperature difference are sequentially transmitted to a digital voltmeter and printer for recording. Following the measurement cycle, the difference between the peak scattered light signal and the previously measured background value is recorded.

A complete 5 min sequence consists of measurements at five supersaturations (currently programmed for 0.25, 0.35, 0.5, 0.75 and 1.0% but readily adjustable to other S values). The operator may also select a control sequence which allows for two measurements at each supersaturation which offers the opportunity of averaging short-time fluctuations in CCN concentration. An internal clock allows spectra to be obtained at any desired intervals from 5 min to several hours. Manual operation for specific experimental purposes is also an option.

4. Calibration

To test the system and determine the gain factors as a function of supersaturation, a calibration was performed against the usual photographic method. Over a period of several days, CCN spectra were measured simul-

TABLE 1. Scattered light sensitivities.

Supersaturation (%)	0.25	0.35	0.50	0.75	1.00
Sensitivity (mV per drop)	0.415	0.511	0.651	0.735	0.869

taneously by the photographic method and also the scattered light technique. It is desirable to perform the measurements over a range of conditions that give nucleus counts over concentration limits anticipated. Figs. 2a–2c are plots of the scattered light signal E_{sc} against the photographic count of CCN concentration for three values of supersaturation. Also plotted (with governing equation) is the least-squares fit to the observations. As can be seen from the figures, the scattered light signal is linearly related to the concentrations indicated by the photographic method. At all supersaturations, virtually all of the observations are within 10% of the best-fit straight line.

Table 1 lists the scattered light sensitivities in terms of signal amplitude (mV) per drop in the scattering volume as a function of supersaturation. A least-squares analysis of the sensitivity as a function of supersaturation resulted in the power function

$$F=0.13S^{0.55},$$

where F is the ratio of the scattered light E_{sc} to the CCN concentration. The exponent agrees favorably with the detailed model prediction of 0.57. This supersaturation dependence can be expected to vary somewhat with individual chamber design. An error analysis indicates that for typical aerosol spectra ($k=0.5$–1.0) the overall measurement error is approximately $\pm 10\%$ at 1% S and $\pm 15\%$ at 0.25% S.

The photographic method of operating the thermal-gradient chamber has the same advantages and limitations as described elsewhere (Twomey, 1967; Squires, 1972; Jiusto, 1976; Alofs and Carstens, 1976). As the latter authors suggest, such instruments may possess more reliable relative rather than absolute value information. In the optical scattering mode described, the customary limitations still hold. Detection of drops and CCN count repeatability appear to improve somewhat. The departure from monodisperse drop sizes at low S, as mentioned, is more critical with the light scattering method.

5. System application

Fig. 3 is a selected 4-day segment of hourly data taken with the light scattering CCN system showing the time variation of the concentration and slope parameters (C and k, respectively) for the spectra $N=CS^k$. [Note that C is equal to the concentration (cm^{-3}) of CCN at $S=1\%$.]

On the first day, the passage of a cold front and associated change of air mass appears as a sharp decrease in the CCN concentration from about 4000 to

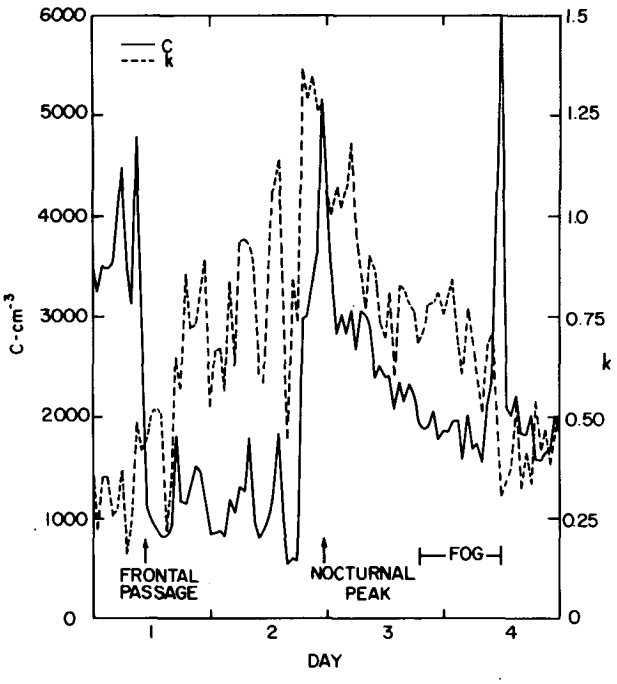

FIG. 3. CCN spectra data from a selected 4-day period of hourly measurements. Solid curve and left ordinate are for the spectrum concentration factor C and the broken curve and right hand ordinate are for the spectrum slope parameter k. Local midnights are indicated along the abscissa.

1000 cm^{-3} over a 4 h period. The slopes of the spectra, however, show a slight increase during this period. The five days following the front were characterized by clear weather with winds primarily from a southerly direction. The second event of interest is the occurrence of a night peak on the second day of the sequence at about 2300 p.m. During the 5 h preceding the peak, the concentration rises from about 600 cm^{-3} to over 5000 cm^{-3}, while the slope changes from 0.4 to 1.3. Lee and Jiusto (1974) in an experiment primarily concerned with the phenomena of the nocturnal peaks noted similar local occurrences in approximately one-third of their daily data. The phenomenon was first noted in Australia by Twomey and Davidson (1970). A third major event occurred during days 3 and 4 of the sequence. At about 2000 on day 3 a fog formed which lasted through noon of the next day. The interesting segment of data is the strong increase in the CCN concentration during the dissipating stage of the fog (0900 to noon on day 4). During this time the concentration rapidly increased from 1500 cm^{-3} to over 6000 cm^{-3}, while the slope decreased from 0.7 to 0.3. A possible explanation for this result is that the evaporation of the fog drops resulted in the production of cloud nuclei either through some chemical reaction or by some type of nucleus breakup mechanism. The short life of the high concentrations is probably due to mixing by convection following the dissipation of the fog.

As the data clearly show, there are substantial temporal variations in the CCN spectra which would be missed if observations were made at longer time intervals. Clearly, the ability to measure the CCN spectra with good time resolution will be a valuable tool for studying the effect of large scale and local influences on CCN.

6. Summary

The design and principle of operation of a continuous CCN counter have been described. The main features of the system are 1) the use of a thermal gradient diffusion chamber in which supersaturation is accurately prescribed; 2) a compact shallow chamber with a short time to reach equilibrium at sequential supersaturations; 3) the automatic measurement of the droplet concentration by means of scattered light; 4) the capability of direct calibration by means of the usual photographic method; and 5) the ability to measure and record CCN spectra at fixed time intervals without the presence of an operator.

The instrument has been operated for long periods of time without interruption showing that it can be used for routine observations of detailed temporal variations in CCN. Extended field studies using the instrument are underway. To date the associated advantages of automation and reduction of data analysis time far outweigh any accuracy constraints described.

Acknowledgment. This research was sponsored by the Atmospheric Research Section of the National Science Foundation under Grant DES73-00410-A01.

REFERENCES

Alofs, D. J., and J. C. Carstens, 1976: Numerical simulation of a widely used cloud nucleus counter. *J. Appl. Meteor.*, **15**, 350–354.

Hodkinson, J. R., and J. R. Greenfield, 1965: Response calculations for light-scattering aerosol counters and photometers. *Appl. Opt.* **4**, 1463–1474.

Jiusto, J. E., 1976: Cloud condensation nucleus counters. *Atmospheric Technology*, NCAR, No. 8, 43–49.

Lee, T. D., and J. E. Jiusto, 1974: Diurnal variations in cloud condensation nuclei. *J. Geophys. Res.*, **79**, 5651–5656.

Radke, L., and P. Hobbs, 1969: An automatic CCN counter. *J. Appl. Meteor.*, **8**, 105–109.

Squires, P., 1972: Diffusion chamber for measurement of cloud nuclei. *J. Rech. Atmos.*, **6**, 565–572.

Twomey, S., 1967: Remarks on the photographic counting of cloud nuclei. *J. Rech. Atmos.*, **3**, 85–90.

Twomey S., and K. A. Davidson, 1970: Automatic observations of cloud nucleus concentrations. *J. Atmos. Sci.*, **27**, 1056–1059.